Journal of Applied Polymer Science

Millimeter-size polyethylene hollow spheres synthesized with $MgCl_2$-supported Ziegler-Natta catalyst

Meizhou Qi, Biao Zhang, Zhisheng Fu, Junting Xu, Zhiqiang Fan
MOE Key Laboratory of Macromolecular Synthesis and Functionalization, Department of Polymer Science and Engineering, Zhejiang University, Hangzhou 310027, China
Correspondence to: Z. Fan (E-mail: fanzq@zju.edu.cn)

ABSTRACT: Polyethylene hollow spheres with diameters of 0.4–2 mm were synthesized by a two-step slurry polymerization in a single reactor with a spherical $MgCl_2$-supported Ziegler-Natta catalyst activated by triethylaluminum, in which the first step was prepolymerization with 0.1 MPa propylene and the second step was ethylene polymerization under 0.6 MPa. The prepolymerization step was found necessary for the formation of hollow spherical particles with regular shape (perfectly spherical shape). The effects of adding small amount of propylene (propylene/ethylene < 0.1 mol/mol) in the reactor after the prepolymerization step were investigated. Average size of the polymer particles was increased, and the polymerization rate was markedly enhanced by the added propylene. Development of the particle morphology with polymerization time was also studied. The polymer particles formed by less than 20 min of ethylene polymerization showed hollow spherical morphology with thin shell layer. Most of the particles had ratio of shell thickness/particle radius smaller than 0.5. By prolonging the ethylene polymerization, the shell thickness/particle radius ratio gradually approached 1, and the central void tended to disappear. Central void in polymer particles formed from smaller catalyst particles disappeared after shorter time of polymerization than those formed from bigger catalyst particles. The shell layer of the hollow particles contained large number of macro-, meso- and micro-pores. The mesopore size distributions of four typical samples were analyzed by nitrogen adsorption–desorption experiments. A simplified multigrain model was proposed to explain the morphogenesis of the hollow spherical particles. © 2015 Wiley Periodicals, Inc. J. Appl. Polym. Sci. **2016**, *133*, 43207.

KEYWORDS: manufacturing; morphology; polyolefins; porous materials; synthesis and processing

Received 11 August 2015; accepted 10 November 2015
DOI: 10.1002/app.43207

INTRODUCTION

Structural and morphological studies on nascent polyolefin particles formed in Ziegler-Natta polymerization have received considerable attentions, as the particle morphology strongly influence the polymerization kinetics, the degree of reactor fouling and the structure as well as properties of the polyolefin materials.[1–17] Different models describing the formation of polyolefin particle morphology have been proposed in the last decades, among which the multigrain model and the polymer flow model are the most popular.[3] In olefin polymerization with heterogeneous Ziegler-Natta catalysts or immobilized metallocene catalysts, the most commonly observed particle morphologies are spherical or near spherical particles with relatively compact shell layer and relatively loose central part. By uniformly immobilize metallocene catalyst inside spherical polystyrene beads and polymerization ethylene with the supported catalyst, Roscoe *et al.* prepared millimeter-size polyethylene (PE) beads with rather homogeneous internal structure and narrow size distribution.[18] Polyethylene particles with onion-like multilayer morphology have been prepared with polymer-supported metallocene catalysts in gas-phase polymerization process.[19] In some cases, nascent polymer particles with large void in the core part were observed.[10,13–15] The multilevel structure of the catalyst particles and severe diffusion limitation to the polymerization reactions in the catalyst-polymer granules were thought as the main causes for such morphology.[3,4] However, it is still difficult to prepare polyolefin particles with regular hollow spherical morphology. The details of the formation mechanism of such hollow spheres have not yet been disclosed in the past.

In recent years, preparation and properties of hollow or multihollow polymer spheres or beads have received increasing attentions.[20–26] Applications of these materials include absorbents, carriers of drug delivery systems, supports of catalysts, sound absorption materials and thermal insulation materials. Because of the highly hydrophobic and partially crystalline characters of polyolefin materials, hollow spheres based on polyolefins may present more interesting properties and find new applications as compared to the hollow spheres based on polar polymers and amorphous

polymers. It is necessary to find better ways of preparing polyolefin-based hollow spheres with regular particle morphology.

In the present work, PE hollow spheres with porous shell layer were prepared through ethylene slurry polymerization with a spherical Z-N catalyst in the presence of propylene. The effects of varied experimental conditions such as prepolymerization, amount of propylene as the comonomer and polymerization time on the morphology of the obtained polymer particles were investigated. The conditions for preparing PE hollow spheres with optimum morphology were identified.

EXPERIMENTAL

Materials

All manipulations involving air-and/or moisture-sensitive compounds were handled under an inert atmosphere of nitrogen using standard Schlenk lines and glovebox. Trimethylaluminum solution (TEA, Albermarle) were obtained commercially and used without further purification. Solutions of TEA (1 mol/L) were prepared by dilution with *n*-heptane before use. *n*-Heptane was distilled from sodium under nitrogen. A high-yield spherical $TiCl_4/MgCl_2$-ID (where ID is an internal donor) catalyst was donated by the Beijing Research Institute of Chemical Industry, Beijing, China. The catalyst contained 2.91 wt % Ti. Polymerization-grade ethylene and propylene were supplied by Yangzi Petrochemical Company (Nanjing, China) and further purified by passing through columns of 4A molecular sieves and deoxygenation catalyst.

Polymerization

The polymer were synthesized in a two-stage polymerization process with a $MgCl_2$-supported Ziegler-Natta catalyst. A 300 mL Büchi autoclave equipped with mechanical stirrer, mass flow meter and a temperature control unit were used as the reactor. The reactor was heated to 90°C for more than 2 h, and repeatedly pressurized with nitrogen, purged and evacuated before polymerization. Then, the temperature was reduced to the prepolymerization temperature (40°C). Prescribed amount of *n*-heptane (100 mL) was added into the reactor under nitrogen atmosphere. The solvent was then saturated by propylene at 0.1 MPa. In the prepolymerization stage, slurry polymerization of propylene was started by adding the catalyst after injection of triethylaluminum (TEA) as cocatalyst. The stirring speed was set at 300 rpm. After 10 min of prepolymerization, the temperature was increased to 65°C and additional amount of propylene was added to the reactor. Immediately after this operation, ethylene at 0.6 MPa was introduced to start the main polymerization stage. Ethylene at 0.6 MPa was continuously supplied to the reactor during the main polymerization. At the end of this stage, the reactor was rapidly vented, and the formed polymer particles were precipitated and washed with acidified (5 wt % hydrochloric acid) ethanol, filtered, and dried at 50°C under vacuum for 12 h.

Fractionation of Pristine Polymer Particles

The polymerization products were extracted with 250 mL boiling *n*-heptane for 24 h in Kumagawa extractor. Then the *n*-heptane soluble part (C7-soluble part or EP, where "C7" means heptane and EP was the abbreviation of ethylene-propylene copolymer) was recovered by rotating evaporation and precipitation in ethanol. Both the *n*-heptane insoluble part (C7-insoluble part) and *n*-heptane soluble part were dried in vacuum.

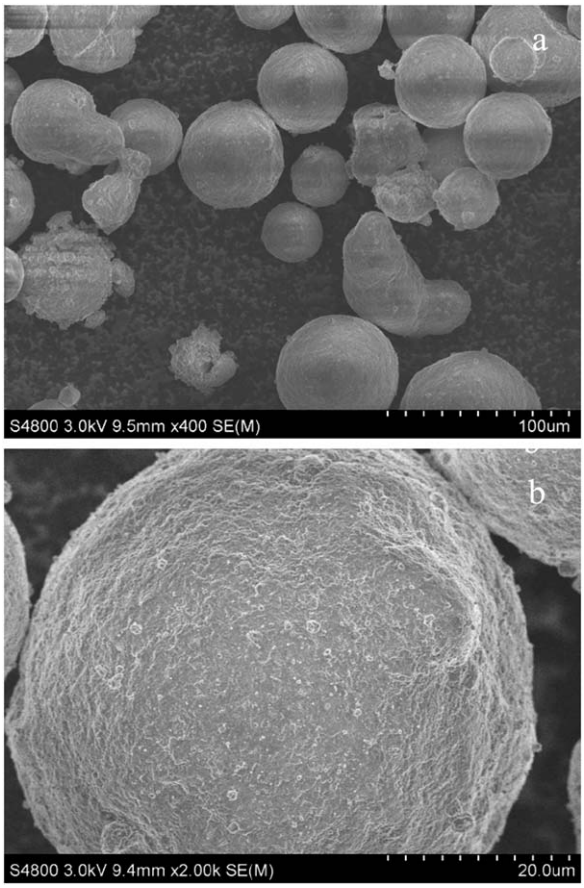

Figure 1. Morphology of pristine catalyst particles observed by SEM (a) The whole particles; (b) Enlarged picture of a particle.

Thermal Analysis of the Fractions

Differential scanning calorimetry (DSC) analysis of the polymers were made by a TA Q200 DSC instrument under N_2 atmosphere. About 5 mg of sample was sealed in aluminum sample pan, and the sample was heated from 30°C to 180°C at a heating rate of 10°C/min and kept melting for 5 min, and then the sample was cooled down to 40°C. Finally, the melting endotherm of the sample was recorded at a heating rate of 10°C/min from 40°C to 150°C.

Measurement of Molecular Weight

The molecular weight and molecular weight distribution of the polymer samples were measured by gel permeation chromatography (GPC) in a PL 220 GPC instrument (Polymer Laboratories). The analysis was performed at 150°C using 1,2, 4-trichlorobenzene as the solvent at a flow rate of 1.0 mL/min. The columns were calibrated with polystyrene standards.

Morphology Analysis

Scanning electron microscope observations of the catalyst, prepolymer and PE particles were made with a Hitachi-4800 SEM. Micrographs were taken at 3-kV acceleration voltage. Before SEM observations, all the sample surfaces were coated with a

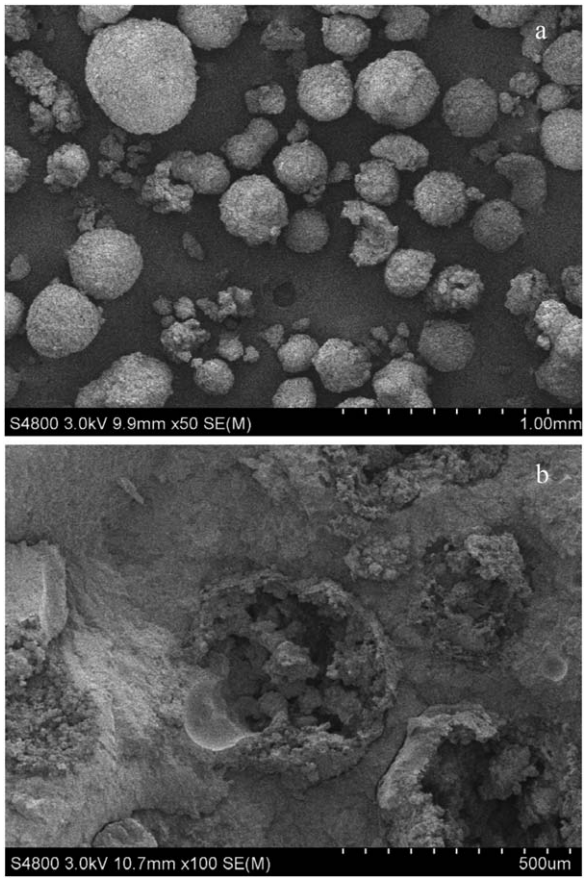

Figure 2. SEM pictures of PE particles prepared without prepolymerization (a) The whole particles; (b) Sectioned PE particles imbedded in cured epoxy resin. Polymerization conditions: *n*-heptane = 200 mL; Al/Ti = 120 (mol/mol); temperature = 65°C; time = 30 min; ethylene pressure = 0.6 MPa.

thin layer of gold. Sectioned polymer particles for SEM or optical microscopy observation were prepared by cutting the particle using a sharp blade, or by sealing the whole particles in epoxy resin and breaking the stick of cured epoxy resin in liquid nitrogen. Morphology of some sectioned polymer particles were observed with a XJZ-6 polarized optical microscopy (POM).

N_2 Adsorption–Desorption Isotherm Curve

Nitrogen adsorption–desorption isotherms and pore-size distributions of the PE particles were measured using an AUTOSORB-1-C instrument (Quantachrome, USA) at 77 K. Prior to the experiments, the samples were degassed in vacuum at 65°C for 24 h. Their specific surface areas were determined on the basis of BET (Brunauer-Emmett-Teller) adsorption model. The total pore volumes and average pore sizes were also calculated. The pore size distributions were statistically obtained by using a Quantachrome software following BJH theory according to the desorption isotherms.

RESULTS AND DISCUSSION

Influence of Prepolymerization on Ethylene Polymerization

It is widely accepted that the morphology of crystalline polyolefin particles is mainly determined by the morphology of the catalyst particles through replication phenomenon.[27–29] Thus, it is necessary to observe the catalyst morphology in advance. Morphology of the catalyst used in this work was examined with SEM (see Figure 1). The catalysts were generally spherical in shape, with a not so broad particle size distribution mainly ranging from 20 μm to 50 μm, though there were also some irregular particles and fragments.

After direct ethylene polymerization under 0.6 MPa without prepolymerization, very low catalytic activity (about 2.0 kg polymer/(g

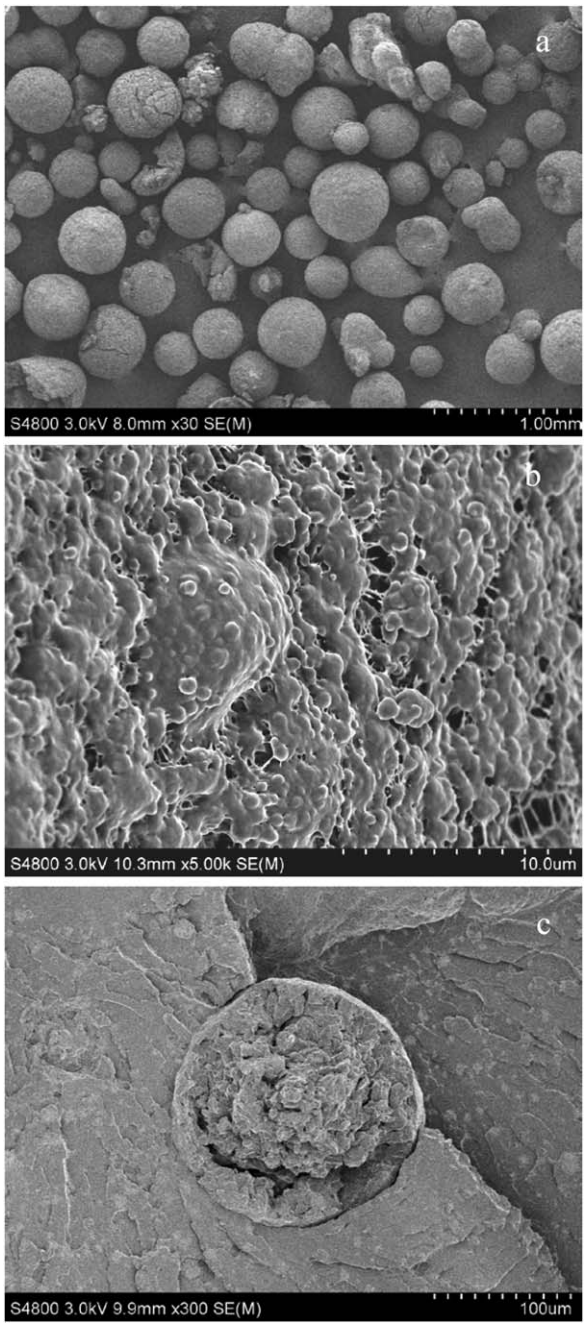

Figure 3. Morphology of prepolymer particles observed by SEM (a) The whole particles; (b) Enlarged area on the surface of a particle; (c) Surface of a sectioned particle imbedded in epoxy resin. Polymerization conditions: *n*-heptane = 200 mL; Al/Ti = 120 (mol/mol); temperature = 40°C; time = 10 min; Propylene pressure = 0.1 MPa.

Table I. Effect of the Amount of Additional Propylene as Comonomer on Catalytic Activity and Polymer Properties[a]

Entry	Propylene[b] (mmol)	Activity (kg/g Ti·h·bar)	EP[c] (wt %)	M_w[d] (kg/mol)	PDI[d]	T_m[e] (°C)	ΔH_m[e] (J/g)
P[f]	0	18.0	0	963	7.9	125.1	110.6
P0[g]	0	26.0	9.1	522	7.3	123.1	100.8
P1	2.4	43. 1	6.2	637	6.3	122.6	103.6
P2	4.0	57.0	8.2	696	4.7	123.0	107.9
P3	5.6	65.6	10.0	715	5.7	123.5	102.0
P4	7.2	79.0	12.8	740	4.6	122.9	103.7
P5	8.8	77.6	17.6	715	5.0	122.5	99.5
P6	10.4	73.2	28.0	696	5.3	122.2	90.0

[a] Polymerization conditions: *n*-heptane = 200 mL; Al/Ti = 120 (mol/mol); Prepolymerization temperature = 40°C; Prepolymerization time = 10 min; Main polymerization temperature = 65°C; Main polymerization time = 30 min; Ethylene pressure = 0.6 MPa.
[b] Amount of propylene added after the prepolymerization step before introducing ethylene. The amount of ethylene in the reactor at the beginning of the main reaction was about 120 mmol.
[c] The boiling *n*-heptane soluble part of product.
[d] Weight average molecular weight and polydispersity index of the part of products insoluble in boiling *n*-heptane.
[e] Melting temperature (T_m) and melting enthalpy (ΔH_m) of the boiling *n*-heptane insoluble part measured by DSC.
[f] Most of propylene in the reactor was removed after the prepolymerization step and no more proplene was added before introducing ethylene.
[g] Remaining propylene in the reactor was not removed after the prepolymerization step, but no more propylene was added before introducing ethylene.

Ti·h·bar)) was obtained, and the size of polymer particles was only 100-300 μm as shown in Figure 2(a). As shown in Figure 2(b), the particles had very loose internal structure, with irregular macro voids in the core part. Meanwhile, many particles were broken, meaning that the pristine polymer particles were not strong enough to withstand the stress caused by the growth of polymer phase, release of reaction heat and collisions between the particles.

When prepolymerization using propylene as the monomer under mild conditions was conducted, the obtained prepolymer were mostly spherical particles of diameter 200–500 μm as shown in Figure 3(a), suggesting that the original shape of the catalysts has been largely retained. Enlarged surface of the prepolymer particle [Figure 3(b)] shows that the surface was rather smooth, and there were tiny holes with size of about 1 μm. The morphology of a sectioned particle [Figure 3(c)] showed rather dense polymer phase in the core part with some macro cracks. Such kind of particle morphology will ensure further penetration of monomers into the particle, but the rate of monomer diffusion will be strongly limited.

A special ethylene polymerization after the prepolymerization was conducted by first withdrawing most of the remaining propylene in the reactor and then introducing ethylene of 0.6 MPa. In this case, the catalytic activity was found to be about nine times higher than that without prepolymerization (see Table I Entry P). This strong activation effect could be attributed to the so-called comonomer effect, which has been reported in literatures before.[30–35] The SEM pictures of typical PE particles are shown in Figure 4. It is seen that size of the biggest particle was about 1.5 mm [Figure 4(a)], which was five times bigger than that of the biggest PE particles produced without prepolymerization. It is noted that the particles showed spherical shape with slightly rough surface, and most of the particles has hollow structure with a nearly spherical void in the center [Figure 4(b)]. It can also be seen that the shell layer of the hollow particles was rather porous, with many tiny cracks and voids.

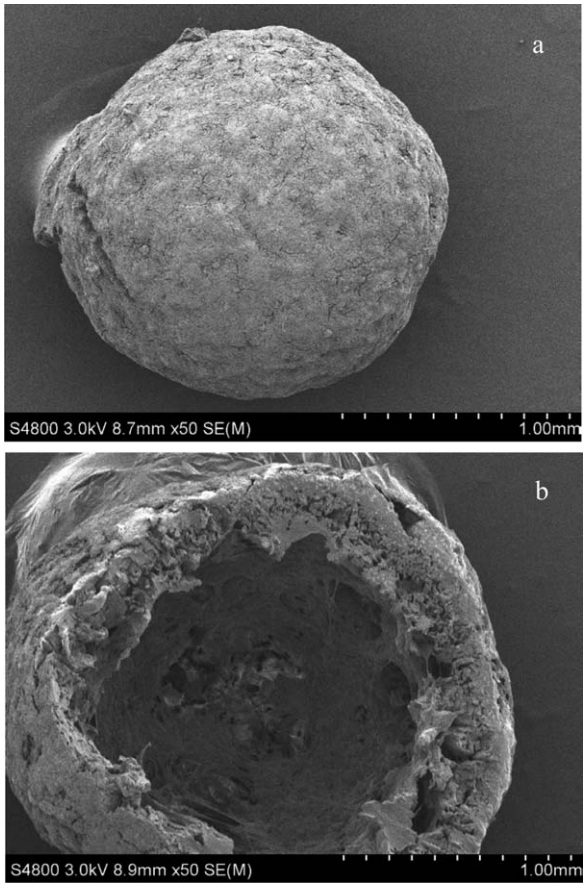

Figure 4. Polyethylene particles prepared with prepolymerization (sample P) (a) The whole particle; (b) Section morphology of a particle cut with a blade. Polymerization conditions: *n*-heptane = 200 mL; Al/Ti = 120 (mol/mol); temperature = 65°C; time = 30 min; ethylene pressure = 0.6 MPa (The conditions of prepolymerization are the same as Figure 3).

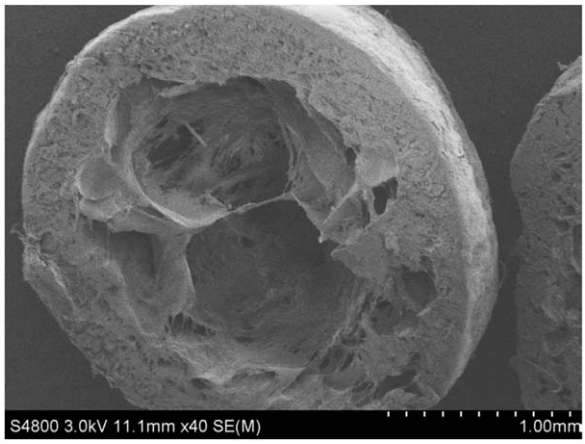

Figure 5. SEM picture of a sectioned pristine particle of sample P4.

From the above mentioned results, it is clear that the prepolymerization step played key roles in enhancing activity of ethylene polymerization and controlling the morphology of polymer particles. Millimeter-size PE hollow spheres with porous shell structure and rather uniform shell thickness can be prepared in a single reactor.

Effect of Propylene as Comonomer on the Polymerization

In our previous works, increasing the concentration of α-olefin comonomer was found to continuously increase the activity of ethylene/α-olefin copolymerization with a supported Z-N catalyst.[34,35] On the other hand, increasing the comonomer content in ethylene/α-olefin copolymer will reduce its crystallinity,[35] thus changing the physical and morphological characteristics of the polymer particles. In this section, we studied the effects of adding designed amount of propylene into the reactor after the prepolymerization step just before introducing ethylene. A series of ethylene/propylene copolymerization runs were thus conducted with different amount of added propylene. The copolymerization results were summarized in Table I. The products (except sample P) were all extracted with boiling *n*-heptane for 24 h to separate the copolymer chains with relatively high propylene content (the C7-soluble part) from the polymer chains with no propylene or with low propylene content (the C7-insoluble part). It is seen that the polymerization activity was continuously enhanced by increasing the amount of propylene until it exceeded 7.2 mmol. Decrease of activity at relatively high propylene concentration may be explained by blocking of the tiny holes on the polymer particles by non-crystalline copolymer, which limits the diffusion of monomer into the particles. As shown in Table I, the amount of copolymer of low crystallinity (the part soluble in boiling *n*-heptane) kept increase with increasing propylene feed.

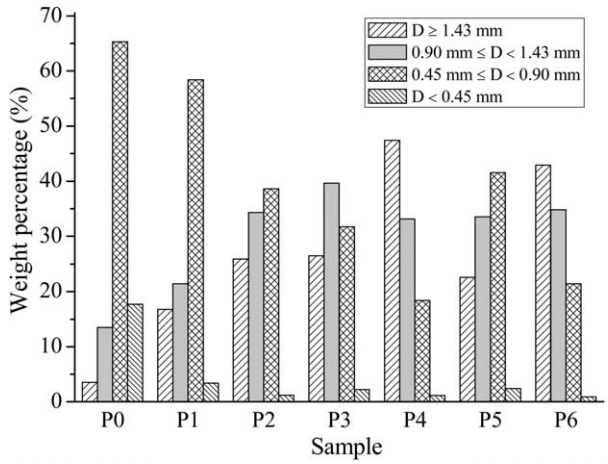

Figure 6. Size distribution of PE particles synthesized at different amount of additional propylene.

The molecular weight of C7-insoluble part was determined by GPC and the results were displayed in Table I. The continuous decrease of both weight average and weight average molecular weight of the C7-insoluble part with increasing propylene amount can be explained by the increase of C7-soluble part, as the C7-soluble part is composed of copolymer with higher propylene content and lower molecular weight.[34] When the amount of propylene exceeded 7.2 mmol (Entries P4-P6), the molecular weight of the C7-insoluble parts tended to decrease, because their propylene content was increased. As an indication of the propylene content, ΔH_m of the C7-insoluble parts decreased from 103.7 J/g of sample P4 to 90.0 J/g of sample P6.

The polymer particles with diameter larger than 0.9 mm synthesized under different propylene concentrations all showed hollow spherical morphology. As shown in Figure 5, a pristine particle of sample P4 had hollow spherical morphology similar to that of sample P [see Figure 4(b)], meaning that hollow spherical particles can be formed even at much higher polymerization rate and when the polymer contains more ethylene-propylene copolymer. The flakes in the void of the particle could be formed by copolymer of high propylene content that is extracted by the solvent during the polymerization. It can be seen that the shell layer of the particle was still highly porous.

Figure 6 shows the size distribution of PE particles synthesized at different amount of additional propylene. By sieving the PE particles into four portions with three sample sieves of different mesh size and then weighing each portion, weight percentages of the

Table II. Effect of Reaction Time on Polymer Yield and Properties[a]

Entry	t_P[b] (min)	Yield[c]	EP[d] (wt %)	M_w[e] (kg/mol)	PDI[e]	T_m[e] (°C)	ΔH_m[e] (J/g)
t10	10	11.0	17.3	513	3.3	121.8	88.6
t20	20	23.8	14.7	632	3.4	122.6	95.3
t30	30	39.5	12.9	740	4.6	122.9	103.7
t40	40	47.8	12.3	783	5.3	124.6	105.0
t50	50	49.7	12.3	822	5.7	124.6	110.7
t90	90	61.0	12.1	1113	5.8	125.2	108.6

[a] Reaction conditions: *n*-heptane = 200 mL, Al/Ti = 120 (mol/mol); Prepolymerization time = 10 min; Prepolymerization temperature = 40°C; Main polymerization temperature = 65°C; Ethylene pressure = 0.6 MPa; Amount of propylene added after prepolymerization = 7.2 mmol.
[b] Polymerization time.
[c] Polymer yield per gram of Ti in kg/(g Ti·bar).
[d] The part of product soluble in boiling *n*-heptane.
[e] Meaning of the parameters are the same as in Table I. The data were obtained from the part of products insoluble in boiling *n*-heptane.

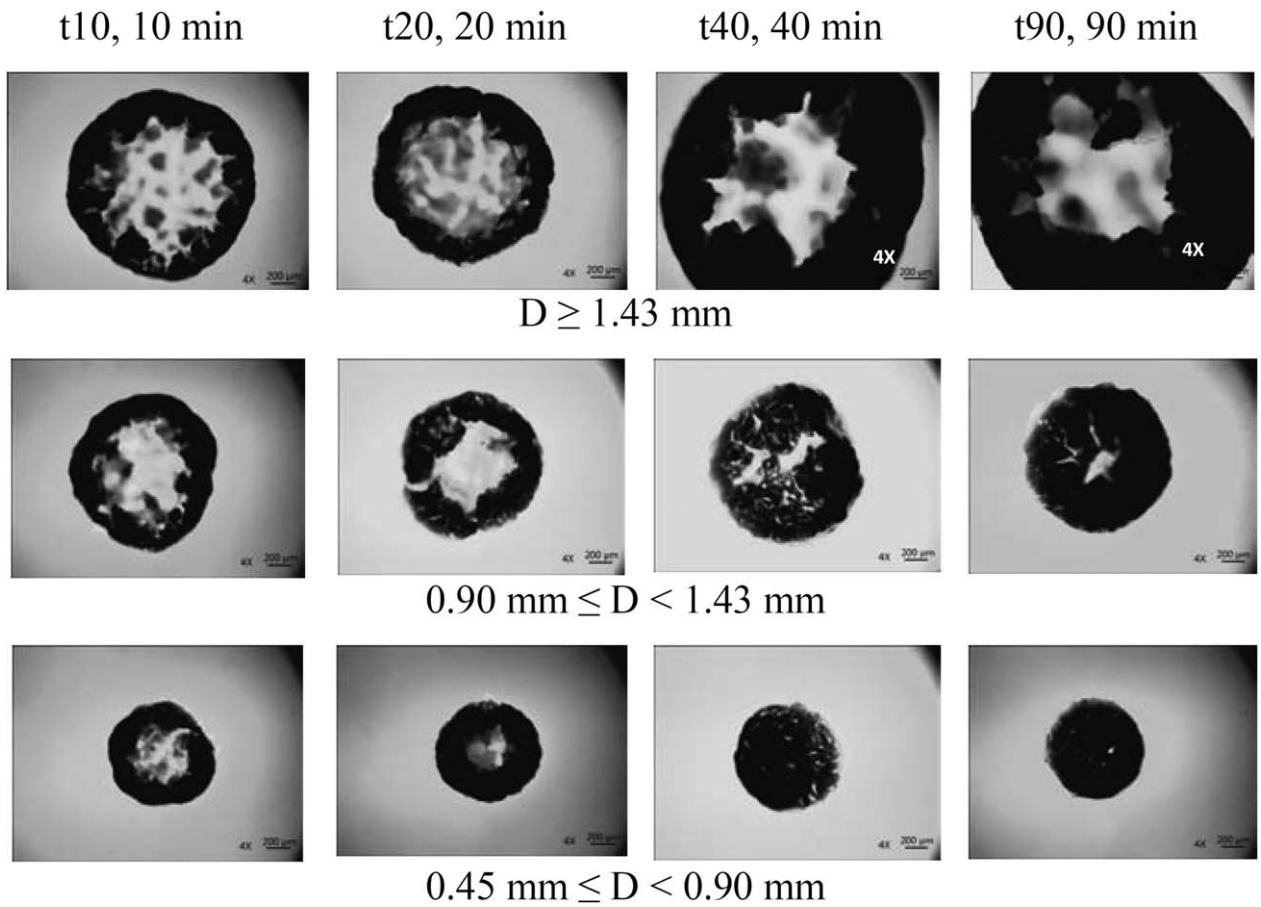

Figure 7. POM pictures of sectioned PE particles of three size ranges ($D \geq 1.43$ mm, 0.90 mm $\leq D <$ 1.43 mm, 0.45 mm $\leq D <$ 0.90 mm) that were formed at different polymerization time. All the pictures were taken at the same magnification. The polymerization conditions are shown in Table II.

four portions of particles from each sample were determined. It is seen that the size distribution continuously shifted to the direction of large size as the polymerization activity increased from sample P0 to P4. The size distributions were not very broad, thanks to the rather narrow size distribution of the catalyst particles.

Effect of Polymerization Time

The effects of increasing polymerization time on the polymer particle morphology have also been studied in this work. Table II summarizes the effects of reaction time on polymerization activity and polymer properties. With increasing the reaction time, the polymer yield increased almost linearly in the first 30 min, and then the polymerization rate decayed rapidly. Besides the decays of polymerization active centers with time, gradual blocking of the tiny holes in the polymer particles by the noncrystalline copolymer may play an important role in reducing the activity, because diffusion barriers to monomer will be sharply increased when the particle porosity decreases. The content of EP decreased initially and then nearly leveled off at a value of 12 wt % from 30 min to 90 min, implying that the active centers capable of incorporating more propylene decay faster than those with lower propylene incorporation rate.[36]

Table II also shows that the molecular weight distribution of C7-insoluble part became broader after 30 min, and polymer of higher molecular weight was formed in the later stage. This could be explained by the decrease of propylene/ethylene ratio with time, as propylene was added to the reactor in one batch, but ethylene was continuously supplied to the reactor. It is well known that molecular weight of ethylene-α-olefin copolymer decreases with increasing α-olefin concentration, as chain transfer to propylene is much faster than that to ethylene in Ziegler-Natta catalysis systems.[34,37] This effect also caused changes in the polymer's thermal properties as a function of polymerization time, as both T_m and ΔH_m gradually increased with time.

The development of particle morphology in the polymerization process was studied by observing the morphology of sectioned particles formed after different time of polymerization. For clarity, the polymer particles of each samples in Table II were sieved into three grades ($D \geq 1.43$ mm, 0.90 mm $\leq D <$ 1.43 mm, 0.45 mm $\leq D <$ 0.90 mm) respectively, and one typical particle was selected from each grade, sectioned and observed by POM. The results are shown in Figure 7. Generally, the biggest particles selected from the grade of $D \geq 1.43$ mm can be regarded as formed by the grade of the biggest catalyst particles. The growth of this grade of particles with time was evident in Figure 7. At short reaction time of 10 min, the particle already formed a clear hollow spherical structure, but thickness of its shell layer was only about 100 μm, and the ratio of

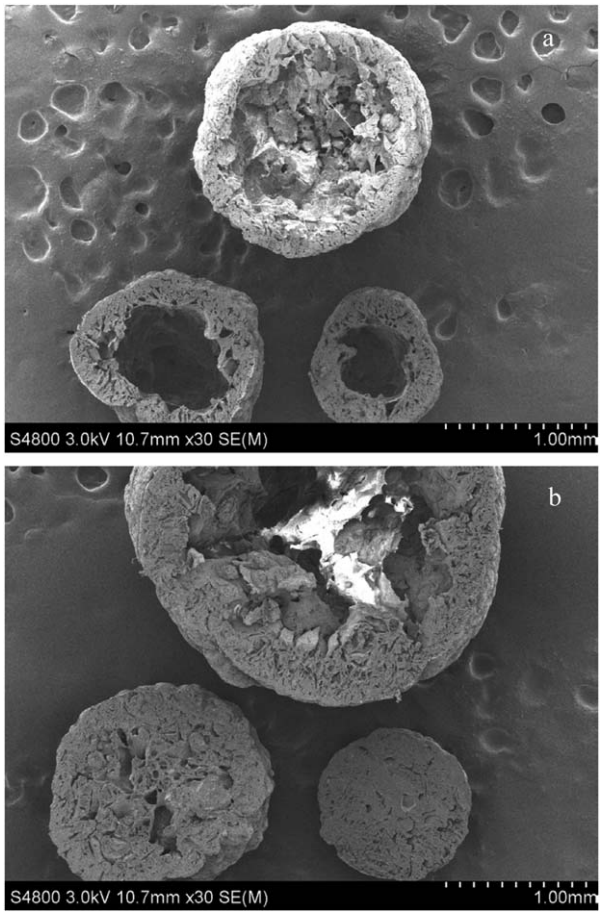

Figure 8. SEM pictures of sectioned PE particles formed after (a) 10 min and (b) 40 min.

shell thickness to particle radius was rather small. With the polymerization time increasing, increasing of the shell thickness was faster than that of the particle radius, leading to reduction of the central void.

For particles of 0.90 mm $\leq D <$ 1.43 mm and 0.45 mm $\leq D <$ 0.90 mm, the same tendency of shell thickening with time can be observed, and the particles formed after 90 min of polymerization were almost compact, especially for the particles of 0.45 mm $\leq D <$ 0.90 mm. This change of particle morphology can be more clearly seen in the SEM pictures (Figure 8). It means that in polymer particles formed from small catalyst particles, the hollow structure may disappear after enough long polymerization reaction.

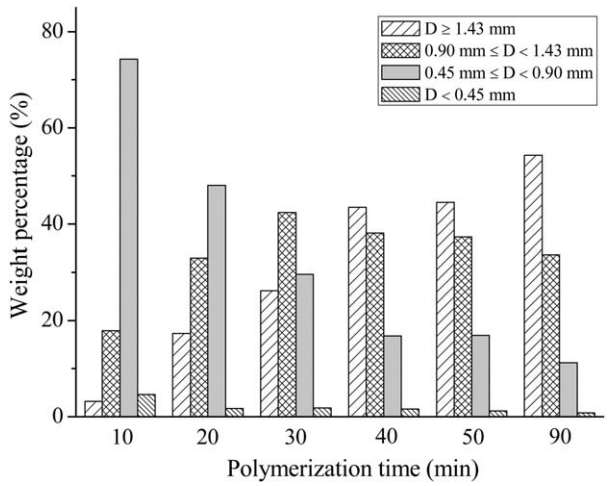

Figure 9. Size distribution of PE particles formed at different reaction time.

Changes of particle size distribution with reaction time are shown in Figure 9. It is clear that percentage of the particles of $D \geq$ 1.43 mm continuously increased with time, those of 0.90 mm $\leq D <$ 1.43 mm increase before 30 min and then tended to decrease, and those of the smallest particles ($D <$ 0.90 mm) decreased with time. Continuous growing of all grades of particles with polymerization time can be concluded from Figure 9.

The development of particle morphology with polymerization time may be qualitatively explained by a simplified multigrain model shown in Figure 10. Before the ethylene polymerization, prepolymerization with propylene was conducted under mild conditions to form catalyst/polymer particles with rather compact surface and internal structure (see Figure 3). When such compact particles meet ethylene in the main polymerization stage, diffusion of ethylene inside the particle will be strongly limited, meanwhile the intrinsic polymerization rate was very high for the high activity of ethylene. This will cause consumption of a large portion of penetrated ethylene in a thin layer just beneath the particle surface. As a result, the active sites on the crystallites of catalyst support in the shell layer can produce more polymer than those in the core part, so the former expands much faster than the latter. Because the crystallites in the core part was covered by only a small amount of polymer, they cannot form a lump with enough strength to withstand the stress exerted by the expanding shell layer, so the core part will be broken into nearly concentric layers attached to the shell layer. Hollow particles thus can be formed in early stage of ethylene polymerization. As the polymerization proceeds, the shell layer will become more compact, and less ethylene will be consumed in the shell layer. Therefore, in the later stage of polymerization, the active sites in the internal part of the particle can receive more ethylene, and the layers near the particle center grows faster than the outer layer, leading to shrinkage of the central void. When the catalyst particles have a relatively smaller size, the distance of ethylene diffusion from the particle surface to the center became shorter, so the core part can receive enough ethylene even in the early stage. This will lead to formation of relatively compact polymer particles without evident central void.

Summarizing the above discussions, formation of hollow spherical PE particles can be realized when the following prerequisites are met:

1. Use spherical catalyst particles with enough large size, suitable friability and porosity;
2. Prepolymerize the catalyst by propylene to form prepolymer particles with relatively compact morphology;
3. Ensure enough high ethylene polymerization rate. The comonomer activation effects can be utilized to enhance the polymerization activity;
4. Duration of the polymerization reaction should not be too long.

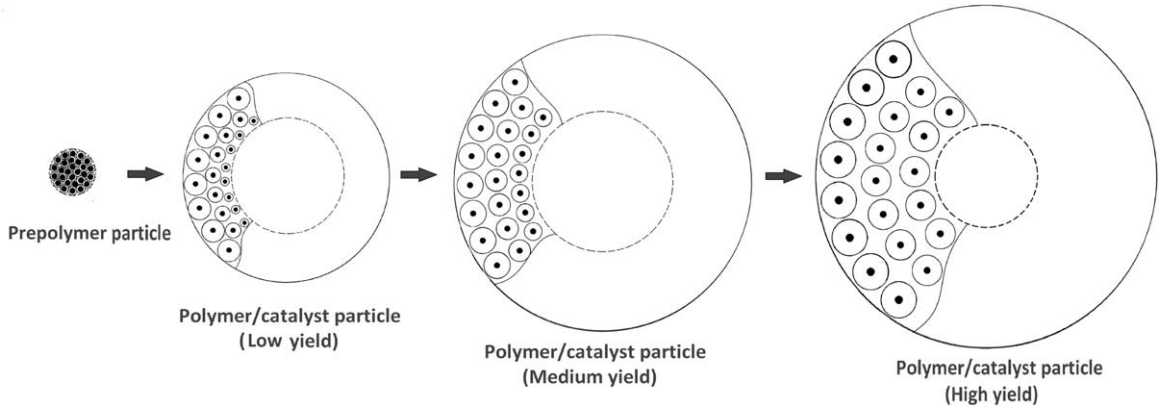

Figure 10. Schematic model of morphogenesis of the hollow polymer particles.

To control the structural parameters of hollow particles such as the ratio of shell thickness to the particle radius, feasible ways include adjusting the duration of polymerization and changing the reaction rate by regulating the ethylene pressure.

The model of morphogenesis proposed here is more or less similar to the models proposed by Nejad *et al.* based on experimental observations[15] and that by Grof *et al.* based on calculations,[38] which are based on multigrain model with strong diffusion limitation. The prioritized growth of the outer shell in the initial stage and the gradual filling of the central void in the later stage of polymerization have been emphasized in our model.

Specific Area and Meso-pores of the Polymer Particles

The solid-phase structure of four PE samples was further analyzed by BET gas adsorption method. The propylene-rich copolymer chains in the nascent particle were removed by extraction in boiling *n*-heptane before the BET analysis. As can be clearly seen from the adsorption–desorption isotherms [see Figure 11(a)], typical IUPAC type-IV isotherm curves can be seen, suggesting the existence of a mesoporous structure. The hysteresis loop in relative pressure (P/P_0) range of 0.8–1.0 for sample P and sample P4 and in P/P_0 of 0.5–1.0 for sample P1 and sample P6 are characteristic of H3-type adsorption. In addition, the hysteresis loop extended to very high P/P_0 value approaching 1, indicating the presence of macropores. Pore size distribution curves of PE particles calculated from the desorption branch of the isotherm showed broad shoulder in the pore size range of >100 nm [Figure 11(b)], which also confirms the presence of macropores. In sample P, there was no mesopores ranging from 19 to 55 nm. In sample P1, the size of mesopores located in 33 to 42 nm. Both samples P4 and P6 had much larger volume of mesopores than the other two samples. Sample P4 also had the largest volume of macropores among the four samples. Considering that the sample P4 was synthesized with the highest activity, it seems that high polymerization rate can increase both mesopores and macropores. A possible reason is that the process of regular pilling the propagation chains to form compact solid-phase may be disturbed by too fast growing of the chains, resulting in more defects in the formed solid structure.

The data of specific surface area and pore volume measured by BET experiments are listed in Table III. Both the specific surface area and the total pore volume changed proportionally with the polymerization activity. Meanwhile, the average pore size decreased with increase of propylene content in the polymer, for polymer chains with higher comonomer content are more flexible than those with lower comonomer content and higher crystallinity.

As seen in Figures 4 and 5, there were large number of macropores of 1 μm or more in the solid-phase of the particles.

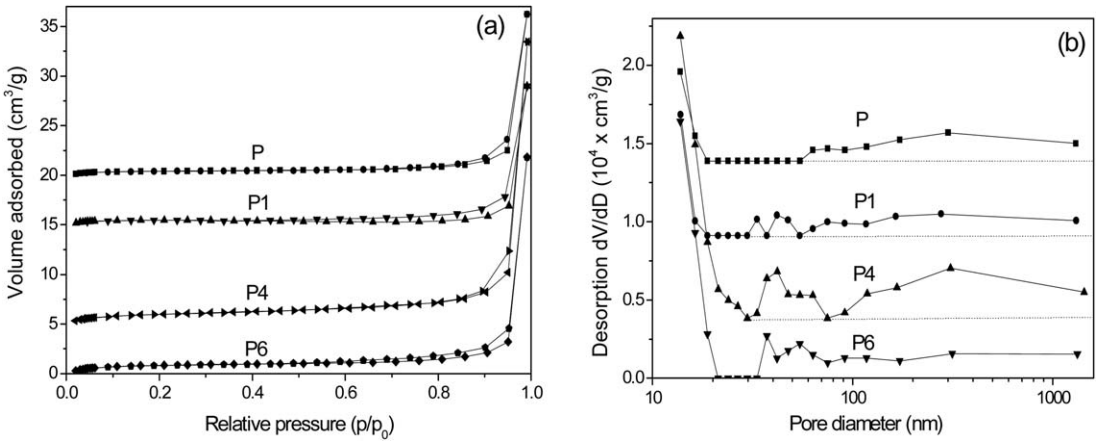

Figure 11. (a) Nitrogen adsorption–desorption isotherms and (b) Corresponding pore size distributions of PE particles.

Table III. Structural parameters of mesopores in PE particles

Sample	Specific surface area (m^2/g)	Total pore volume (mL/g)	Average pore size (nm)
P	1.6	0.025	31.3
P1	1.8	0.022	23.7
P4	4.0	0.044	22.3
P6	3.3	0.034	20.3

These macropores cannot be measured by the BET experiment for the limitation of the method. The solid part of the hollow PE spheres was actually composed of polymer phase (both crystallized and amorphous) containing large number of pores ranging from a few nanometer to several micrometers. In many particles there were also macro cracks that may be caused by occasionally focused stresses during growth of the particle.

In summary, the size and volume of both mesopores and macropores in the hollow PE particles can be regulated by changing the polymerization rate and the amount of comonomer.

CONCLUSIONS

Millimeter-size PE hollow spheres can be synthesized by a two-step slurry polymerization with a spherical $MgCl_2$-supported Ziegler-Natta catalyst, in which the first step was prepolymerization with propylene under 0.1MPa and the second step was ethylene polymerization under 0.6 MPa. The prepolymerization step is necessary to ensure formation of hollow spherical particles with regular shape. Average size of the polymer particles can be increased by adding small amount of propylene in the reactor after the prepolymerization step, as the polymerization rate was markedly enhanced by the added propylene. The polymer particle formed after 10 min of ethylene polymerization showed hollow spherical morphology with thin shell layer and relatively larger central void, or in other words, their ratio of shell thickness/particle radius were small. When ethylene polymerization proceeded for longer time, the ratio gradually approached 1, and the central void tended to disappear. Central void in polymer particles formed from smaller catalyst particles disappeared after shorter time of polymerization than those formed from bigger catalyst particles. Under suitable conditions, namely, ethylene pressure = 0.6 MPa, polymerization temperature = 65°C, and additional amount of propylene = 2–7 mmol, hollow spherical PE particles with diameters of 0.4–2 mm can be synthesized, in which most of the particles have large central void with near spherical shape, and their shell layer contained large number of macro-, meso- and micro-pores.

ACKNOWLEDGMENTS

Supports by National High-tech R&D Program of China (Grant No. 2012AA040305) and National Natural Science Foundation of China (grant no. U1462114) are gratefully acknowledged.

REFERENCES

1. Ingram, P.; Schindler, A. *Die Makromol. Chem.* **1968**, *111*, 267.
2. Blais, P.; Manley, R. S. J. *J Polym. Sci. Part A: Polym. Chem.* **1968**, *6*, 291.
3. McKenna, T. F. L.; Di Martino, A.; Weickert, G.; Soares, J. B. P. *Macromol. React. Eng.* **2010**, *4*, 40.
4. McKenna, T. F. L.; Mattiolli, V. *Macromol. Symp.* **2001**, *173*, 149.
5. Cecchin, G.; Marchetti, E.; Baruzzi, G. *Macromol. Chem. Phys.* **2001**, *202*, 1987.
6. Zheng, X. J.; Pimplapure, M. S.; Weickert, G.; Loos, J. *ePolymers* **2006**, *6*, 356.
7. Debling, J. A.; Ray, W. H. *J Appl. Polym. Sci.* **2001**, *81*, 3085.
8. Hamilton, P.; Luss, D. *Ind. Eng. Chem. Res.* **2008**, *47*, 2905.
9. Thang, V. Q.; Taniike, T.; Umemori, M.; Ikeya, M.; Hiraoka, Y.; Nghia, N. D.; Terano, M. *Macromol. React. Eng.* **2009**, *3*, 467.
10. Hammawa, H.; Wanke, S. E. *J. Appl. Polym. Sci.* **2007**, *104*, 514.
11. Kanellopoulos, V.; Tsiliopoulou, E.; Dompazis, G.; Touloupides, V.; Kiparissides, C. *Ind. Eng. Chem. Res.* **2007**, *46*, 1928.
12. Kanellopoulos, V.; Dompazis, G.; Gustafsson, B.; Kiparissides, C. *Ind. Eng. Chem. Res.* **2004**, *43*, 5166.
13. Fu, Z. S.; Dong, Q.; Li, N.; Fan, Z. Q.; Xu, J. T. *J. Appl. Polym. Sci.* **2006**, *101*, 2136.
14. Fu, Z. S.; Zhang, Y. Z.; Fan, Z. Q.; Xu, J. T. *J. Appl. Polym. Sci.* **2007**, *103*, 2075.
15. Nejad, M. H.; Ferrari, P.; Pennini, G.; Cecchin, G. *J. Appl. Polym. Sci.* **2008**, *108*, 3388.
16. Mehtarani, R.; Fu, Z. S.; Fan, Z. Q.; Tu, S. T.; Feng, L. F. *Ind. Eng. Chem. Res.* **2013**, *52*, 13556.
17. Michler, G. H.; Seydewitz, V.; Buschnakowski, M.; Myasnikowa, L. P.; Ivan'kova, E. M.; Marikhin, V. A.; Boiko, Y. M.; Goerlitz, S. *J. Appl. Polym. Sci.* **2010**, *118*, 866.
18. Roscoe, S. B.; Frechet, J. M. J.; Walzer, J. F.; Dias, A. *J. Sci.* **1998**, *280*, 270.
19. Zhou, J. M.; Li, N. H.; Bu, N. Y.; Lynch, D. T.; Wanke, S. E. *J. Appl. Polym. Sci.* **2003**, *90*, 1319.
20. Zhou, H.; Li, B.; Huang, G. S. *Mater. Lett.* **2006**, *60*, 3451.
21. He, X. D.; Ge, X. W.; Liu, H. R.; Wang, M. Z.; Zhang, Z. C. *J. Polym. Sci. Part A: Polym. Chem.* **2007**, *45*, 933.
22. Ge, X. P.; Ge, X. W.; Wang, M. Z.; Liu, H. R.; Fang, B.; Li, Z.; Yang, C. Z.; Li, G. *Coll. Polym. Sci.* **2012**, *290*, 1749.
23. Kong, X. Z.; Jiang, W. Q.; Jiang, X. B.; Zhu, X. L. *Polym. Chem.* **2013**, *4*, 5776.
24. Fujitsu, Y.; Nakayama, H.; Uchida, T.; Yamazaki, S.; Kimura, K. *J. Polym. Sci. Part A: Polym. Chem.* **2013**, *51*, 780.
25. Jin, J.; Kim, B.; Park, N.; Kang, S.; Park, J. H.; Lee, S. M.; Kim, H. J.; Son, S. U. *Chem. Commun.* **2014**, *50*, 14885.
26. Zhou, H. O.; Shi, T. J.; Zhou, X. *J. Appl. Polym. Sci.* **2014**, *131*, 39761.

27. Huang, R. B.; Liu, D. B.; Wang, S. B.; Mao, B. Q. *Macromol. Chem. Phys.* **2004**, *205*, 966.
28. Xu, R. W.; Liu, D. B.; Wang, S. B.; Mao, B. Q. *Macromol. Chem. Phys.* **2006**, *207*, 779.
29. Wang, J.; Yu, M. S.; Jiang, W. H.; Zhou, Y.; Li, F. J.; Cheng, L.; Yi, J. J.; Huang, Q. G.; Liu, Y. F.; Yang, W. T. *Ind. Eng. Chem. Res.* **2013**, *52*, 17691.
30. Xu, Z. K.; Zhu, Q. Q.; Feng, L. X.; Yang, S. L. *Die Makromol. Chem., Rapid Commun.* **1990**, *11*, 79.
31. Soares, J. B. P.; Hamielec, A. E. *Polymer* **1996**, *37*, 4607.
32. Czaja, K.; Król, B. *J. Appl. Polym. Sci.* **1999**, *71*, 353.
33. Yiagopoulos, A.; Yiannoulakis, H.; Dimos, V.; Kiparissides, C. *Chem. Eng. Sci.* **2001**, *56*, 3979.
34. Yang, H. R.; Zhang, L. T.; Fu, Z. S.; Fan, Z. Q. *J. Appl. Polym. Sci.* **2015**, *132*, 41264.
35. Xu, T.; Yang, H. R.; Fu, Z. S.; Fan, Z. Q. *J. Organomet. Chem.* **2015**, http://dx.doi.org/10.1016/j.jorganchem.2015.04.027
36. Kissin, Y. V.; Mink, R. I.; Nowlin, T. E. *J. Polym. Sci. Part A: Polym. Chem.* **1999**, *37*, 4255.
37. Nikolaeva, M. I.; Matsko, M. A.; Mikenas, T. B.; Echevskaya, L. G.; Zakharov, V. A. *J. Appl. Polym. Sci.* **2012**, *125*, 2042.
38. Grof, Z.; Kosek, J.; Marek, M. *AIChE J.* **2005**, *51*, 2048.